

Particle acceleration in ultra-relativistic oblique shock waves

A. Meli ^{a,b,1} and J.J. Quenby ^a

^a*Astrophysics Group, Blackett Laboratory, Imperial College of Science, Technology and Medicine, Prince Consort Rd. SW7 2BW, London, UK.*

^b*Visiting Max Planck Institut fuer Radioastronomie, Auf dem Huegel 69 53121, Bonn, Germany.*

Abstract

We perform Monte Carlo simulations of diffusive shock acceleration at highly relativistic oblique shock waves. High upstream flow Lorentz gamma factors (Γ) are used, which are relevant to models of ultra relativistic particle shock acceleration in Active Galactic Nuclei (AGN) central engines and relativistic jets and Gamma Ray Burst (GRB) fireballs. We investigate numerically the acceleration properties in the relativistic and ultra relativistic flow regime ($\Gamma \sim 10-10^3$), such as angular distribution, acceleration time constant, particle energy gain versus number of crossings and spectral shapes. We perform calculations for sub-luminal and super-luminal shocks. For the first case, the dependence on whether or not the scattering is pitch angle diffusion or large angle scattering is studied. The large angle model exhibits a distinctive structure in the basic power-law spectrum which is not nearly so obvious for small angle scattering. However, both models yield significant 'speed-up' or faster acceleration rates when compared with the conventional, non-relativistic expression for the time constant, or alternatively with the time scale r_g/c where r_g is Larmor radius. The Γ^2 energization for the first crossing cycle and the significantly large energy gain for subsequent crossings as well as the high 'speed up' factors found, are important in supporting the Vietri and Waxman work on GRB ultra-high energy cosmic ray, neutrino, and gamma-ray output. Secondly, for super-luminal shocks, we calculate the energy gain for a number of different inclinations and the spectral shapes of the accelerated particles are given. In this investigation we consider only large angle scattering, partly because of computational time limitations and partly because this model provides the most favourable situation for acceleration. We use high gamma flows with Lorentz factors in the range 10-40, which are relevant to AGN accretion disks and jet ultra relativistic shock configurations. We closely follow the particle's trajectory along the magnetic field lines during shock crossings where the equivalent of a guiding centre approximation is inappropriate, constantly measuring its phase space co-ordinates in the fluid frames where $\mathbf{E}=0$. We find that a super-luminal 'shock drift' mechanism is less efficient in accelerating particles to the highest energies observed, compared to the first order Fermi acceleration ap-

plying in the sub-luminal case, suggesting that the former cannot stand as a sole acceleration mechanism for the ultra-high energy cosmic rays observed.

1 Introduction

Detection of $10^6 - 10^{20}$ eV nuclei within the solar system, implying their presence through much of the observable universe, has stimulated the development of the diffusive shock acceleration model, whereby particles are repeatedly accelerated in multiple crossings of a shock interface, due to collisions with upstream and downstream magnetic scattering centres. The pioneering work of the late 70s (Krymsky, 1977; Bell, 1978a,b; Axford et al., 1978; Blandford and Ostriker, 1978) established the basic mechanism of particle diffusive acceleration in non-relativistic flows. However, since then, extension of the model to oblique shocks, relativistic plasma flows and the incorporation of non-linear effects, have rendered the emergence of a consensus physical picture more difficult. At oblique shock fronts the motion of the particles is more complicated, compared to a parallel shock configuration, as they may either be transmitted or reflected by the shock surface. Apart from the diffusive acceleration mechanism, an oblique shock could also accelerate particles in the *absence* of scattering (Armstrong and Decker, 1979), and this mechanism is called 'shock drift' acceleration. Provided that the motion of the particles is diffusive in the oblique shock configurations it has been shown, for an analytical non-relativistic flow approach, that the same result as in parallel shocks, connects the power-law index of accelerated particles with the compression ratio and the acceleration rate with the diffusion coefficients in the shock normal direction (e.g. Axford et al., 1978; Bell, 1978a; Drury, 1983).

Also, following energy gain in the shock frame on shock crossing via the drift approach, is equivalent to following the gain via Lorentz transformations from the shock frame into an $\mathbf{E}=0$ frame (defined by de Hoffmann and Teller, 1950) at the shock, and then back into the shock frame. On the other hand, the theory of oblique shocks considers features that are not involved in the parallel shock case, in particular the ability of the shock to reflect particles meeting a weaker to stronger field transition and the dependence of the acceleration time on the field-shock normal angle (e.g. Jokipii, 1982). Oblique shocks can be classified into sub-luminal and super-luminal. The difference between these two categories is that, in the sub-luminal case, it is possible to find a relativistic transformation to the frame of reference (de Hoffmann-Teller frame), in which the shock front is stationary and the electric field is zero ($\mathbf{E}=0$) in both upstream and downstream regions. On the other hand, super-luminal shock

¹ Corresponding author: a.meli@ic.ac.uk

fronts do not admit a transformation to such a frame, as they correspond to shock fronts in which the point of intersection of the front with a magnetic field line moves with a speed greater than c . Kirk and Heavens (1989) employed a numerical solution to the transport equation (in the test particle limit) and found spectral flattening at relativistic speeds in inclined shocks as well as an increased anisotropy both in fluid frames and the $\mathbf{E}=0$ frame. These results were confirmed by Monte Carlo simulations (Ostrowski, 1991 and Lieu et al., 1994). The former author investigated the gyromotion across the shock to check the region of applicability of magnetic moment conservation in the $\mathbf{E}=0$ frame at the shock while, the later authors simply relied on this assumption. Baring et al. (1994) noticed 'bumps' in the accelerated spectra just upstream of the shock in the non-relativistic oblique case. The reason a Monte Carlo approach became favoured, lies in the large anisotropies and gradients which develop around the shock at relativistic flow speeds. These render direct solution of the transport equation difficult, because the Boltzmann equation must be applied to a fine-grained bundle of particle trajectories in phase space and the diffusion approximation, employing a simple spatial diffusion tensor is inadequate (e.g. Axford, 1981).

All the work mentioned so far is sub-luminal, but Bednarz and Ostrowski (1998) used a small-angle scattering model to include super-luminal situations with field-shock normal angles, $\psi \leq \pi/2$ and flow $\Gamma \leq 243$ and also a simulation of varying amounts of cross-field diffusion. These authors found spectral indices which could be very large at intermediate Γ values with small K_{\perp} , but at high Γ , all results appeared to tend towards a differential exponent of -2.2.

Earlier discussion of an extreme example of a super-luminal case, the pulsar wind shock acceleration scheme for the termination shock of an isolated pulsar magnetosphere where the $\Gamma \sim 10^4$ polar wind meets the slowly expanding nebula envelope, has emphasized the apparent difficulty in achieving multiple shock crossings of accelerated particles. This can be seen if we remember that for super-luminal shocks, a transformation to a frame with \mathbf{B} parallel to the shock plane is possible (Hudson, 1965) so in the absence of scattering close to the shock, particles are swept at an angle to the shock normal into the shock, shock drift and then exit downstream with no return possible. Begelman and Kirk (1990) note that only shock compression of the upstream population results in the low turbulence case. However, Lucek and Bell (1994) find special trajectories if the field is ordered but not uniform, allowing energy increases by factors of the order of hundreds per crossing, which coupled with particle motion in the electromagnetic field of the nebula can render isolated pulsars accelerators of high energy cosmic rays. Gallant and Arons (1994) provide a rare example of a hybrid model of relativistic particle acceleration, applied to the Crab Nebula, using a fluid approach for an e^{\pm} pair plasma together with a kinematic treatment of ions to compute the synchrotron spectrum.

Acceleration time under non-relativistic theory clearly depends on shock obliquity through variation of K_n , the diffusion coefficient along the shock normal,

with ψ , where $K_n = K_{\parallel} \cos^2 \psi + K_{\perp} \sin^2 \psi$. K_{\parallel}, K_{\perp} are respectively the diffusion coefficients parallel and perpendicular to the field. The acceleration time is given by,

$$\tau = \frac{3}{V_1 - V_2} \left(\frac{K_{n,1}}{V_1} + \frac{K_{n,2}}{V_2} \right) \quad (1)$$

Here the suffixes '1' and '2' refer to upstream and downstream, and V is plasma flow velocity. Because this equation (1) is clearly an inadequate measure of acceleration time in the highly relativistic case, we note it may also be written as τ lying in the range $(4 \rightarrow 8/3)(nr_g/c)\cos^2\psi$ for a parallel mean free path $\lambda_{\parallel} = nr_g$, a shock frame compression ratio of 4 and a downstream reduction in λ_{\parallel} by a factor 4. Hence while it will be convenient to measure any 'speed-up' of acceleration relative to equation (1), we may equally regard the time to move over the relativistic Larmor radius as the unit of acceleration time for comparison purposes. Quenby and Lieu (1989) and Ellison et al. (1990) employed Monte Carlo guiding centre approximation calculations to show that relativistic parallel shock flows with $\Gamma \sim 10$ produced a 'speed-up' of acceleration by factors $\sim 3 \rightarrow 10$ when compared with equation (1) for τ . The former authors argued for large angle scattering while the latter found essentially the same result with either large or small angle scattering. Lieu et al. (1994) showed the speed-up as a function of flow velocity was similar for inclined, sub-luminal shocks, provided the results are plotted against flow seen in the $\mathbf{E}=0$ frame. Quenby and Drolias (1995) using an inclined shock model which included the expected shock structure due to cosmic ray pressure back reaction, found some speed-up still occurred. Bednarz and Ostrowski (1996) employ a Monte Carlo computation scheme to investigate acceleration times for shock speeds up to $0.9c$ for the inclined case, with both small angle and large angle scattering and allowing for cross field motion of guiding centres. Speed-up is noticed especially at high shock speed and turbulence although, cross-field diffusion eventually reverses the correlation with turbulence level. Power law spectra only occur in the super-luminal case for isotropic scattering. Acceleration time scales, shorter than the upstream gyroperiod have been obtained.

In a companion work, Meli and Quenby (2002a), have studied parallel shock acceleration for flow $\Gamma \leq 10^3$, for both small and large angle scattering models using the guiding centre Monte Carlo approach. They confirm a Γ^2 energy enhancement for the first shock crossing cycle, first emphasized by Quenby and Lieu (1989,) and they find significant energy gains subsequently. Also, the structure in the accelerated particle spectrum at the shock, indicated in previous lower Γ simulations, became enhanced for large angle scattering, although not in the small angle case, rendering the idea of a simple power law output spectrum for photon production uncertain and they confirm the existence of the speed-up effect. It is the purpose of this work to extend the parallel shock studies of Meli and Quenby (2002a) to provide answers con-

cerning the acceleration time scales, particle spectral shape at the source, angular distribution and energy gain per cycle of the accelerated particles for different shock inclinations using very high gamma flows. We consider both sub-luminal shocks (where an $\mathbf{E}=0$ frame can be found) and super-luminal ones (where $\mathbf{E}=0$ is impossible) and the helical particle trajectories are followed in the appropriate frames to determine the characteristics of the shock crossing. Streaming instabilities, drift waves and Rayleigh-Taylor like instabilities all can increase scattering around the shock and contribute to the back reaction of the relativistic gas, but these are not enough to destroy the basic relativistic beaming in flows, where $V \rightarrow c$. Hence a Monte Carlo approach is employed. The speed-up for a true discontinuity in the test-particle strong scattering limit, is due to a $\sim \Gamma^2$ change in energy in one complete shock crossing cycle for shock Γ , and this effect is the basic cause of the deviation of the spectral shape from the non-relativistic result. Our current interest, regarding a real astrophysical scenario, lies in relativistic flows in AGN jets where $\Gamma \approx 5 - 10$ and in GRB fireballs where a $\Gamma \approx 10^2 - 10^3$ is estimated.

2 Numerical Method

In these Monte Carlo codes we use both large angle and pitch angle scattering, assuming elastic scattering in the fluid frames and the important aim is to investigate the role of different scattering models in reference to spectral shape, acceleration time scales and angular distribution in different frames of reference with varying shock obliquity at very high gamma plasma flows, ranging from $\Gamma = 10 - 10^3$. We consider oblique, sub-luminal and super-luminal shocks with $15^\circ \leq \psi \leq 75^\circ$ where ψ is the angle between the shock normal and the magnetic field, seen in the shock frame. The relativistic frames of references we use during the calculations are, the local fluid frame (1,2), the normal shock frame (s) and the de Hoffman-Teller frame (HT). In general, flow into and out of the shock discontinuity is not along the shock normal, but a transformation is possible into the normal shock frame to render the flows along the normal (e.g. Begelman and Kirk, 1990) and for simplicity we assume such a transformation has already been made.

2.1 *Sub-luminal case*

The Monte Carlo codes for the simulations in the sub-luminal case are similar to the treatment we followed in Meli and Quenby (2002a) for the parallel shock simulations, apart from the fact that more complicated relativistic formulas and different frames of references are used (which make the runs of the codes

considerably more CPU-time consuming). First, relativistic particles are injected upstream and are allowed to scatter in either fluid frame and across the shock discontinuity. We follow each particle trajectory across the shock according to the jump conditions and each particle leaves the system when it 'escapes' far downstream at the spatial boundary or if it reaches a well defined maximum energy E_{max} , equal to $10^{10}E_o$. The spatial boundary is placed $\sim 100\lambda$ downstream in the large angle scatter case which proved an optimum number, but for small angle scattering, the possible dependence of the results on this parameter needed investigation (see the 'Results' section). The compression ratio $r = \frac{V_1}{V_2}$ takes the values of 4 and 3 for comparison with previous work with varying relativistic Rankine-Hugoniot conditions and a similar version of Bednarz and Ostrowski (1998) splitting technique is used (see Meli and Quenby, 2002a) so that when an energy is reached such that only a few accelerated particles remain, each particle is replaced by N of statistical weight $1/N$ so as to keep roughly the same number of particles being followed. A guiding centre approximation is used, where the particle trajectory is followed in two-dimensional, pitch angle and distance along \mathbf{B} space. The mean free path is calculated in the respective fluid frames by the formula: $\lambda = \lambda_o p_{1,2}$, assuming a momentum dependence to this mean free path for scattering along the field and related to the spatial diffusion coefficient, K , in the shock normal or x direction by $K_{\parallel} = \lambda v/3$ and $K = K_{\parallel} \cos^2 \psi$. Thus we specifically neglect cross-field diffusion, under conditions to be discussed in the next paragraphs. There are three conditions for the guiding centre approximation to be fulfilled relating to the ratio K_{\perp}/K_{\parallel} , the probability of hitting the shock at the last scattering including the effect of field line wandering near the shock and the across field jumps each scatter and we mention these, employing entirely plasma frame variables. If $K_{\perp}/K_{\parallel} \leq 0.1$, diffusion away from the shock is clearly predominantly along the mean field. Adapting quasi-linear theory for gyro-resonance scattering by a wave number, k , spectrum of fluctuations perpendicular to the mean field of power $P(k) = Ak^{-n}$ we get (Jokipii, 1966),

$$K_{\parallel} = \frac{vB^2 r_g^{2-n}}{\pi(2-n)(4-n)A} \quad (2)$$

To match the usual assumption, $\lambda_{\parallel} \propto r_g$, we need $n=1$. Then if k_o, k_1 are the lower and upper limits to the wave number spectrum, chosen to avoid divergence in fluctuation power,

$$\lambda_{\parallel} = \frac{r_g}{\pi} \frac{\ln(k_1/k_o)}{\delta b^2} \quad (3)$$

where δb^2 is the power in transverse fluctuations normalized to the mean field. Perpendicular diffusion is likely to be predominantly due to field line

wandering with (Jokipii and Parker, 1969),

$$K_{\perp} = \frac{v}{4B^2} P_{\parallel}(k \rightarrow 0) = \frac{v}{4k_{\circ}} \frac{\delta b_{\parallel}^2}{\ln(k_1/k_{\circ})} \quad (4)$$

where $P_{\parallel}(k \rightarrow 0)$ is the power in the parallel field at wave numbers near zero. Even if the fluctuations are isotropic parallel and perpendicular to the field and if $k_{\circ}^{-1} = L_s/2\pi$ where L_s is the scale size of the acceleration region, with $\delta b \sim 0.3$ and $k_1/k_{\circ} \sim 10$, since at the highest reasonable r_g , $r_g \leq L_s/10$, we expect $K_{\perp}/K_{\parallel} \sim 0.05$. Hence at high r_g the guiding centre approximation for the mean field is reasonable.

At low r_g , perpendicular motion is entirely determined by the wandering of the field line bundle to which the particle is 'attached' and it is the local value of ψ , within a few λ_{\parallel} of the shock, which determines the acceleration details. However, a second criterion that the guiding centre approximation remains reasonable is that $\tan\psi \leq \lambda_{\parallel}/r_g$. This means physically that the gyrating particle does not on average scatter far enough off from the original 'bundle' to intersect the shock front, as it scatters at a distance of one parallel mean free path from the front along the actual field line. The reason for the scattering, large angle or a reflection due to multiple small-angle scatterings, is not crucial. For the above parameters this criterion becomes $\psi \leq 84^{\circ}$. However, since the field itself 'wanders' by an rms value $\sim 18^{\circ}$, the guiding centre approximation is probably limited to field-shock normal angles $\leq 66^{\circ}$, at all r_g .

As explained by Baring et al. (1995), each scatter induces a jump across the field which changes the distance to the shock by $\leq r_g$, but this is unimportant in the numerical regime we consider where, $\lambda_{\parallel} \geq 10r_g$.

The probability that a particle will move a distance Δs along the field lines at pitch angle θ before it scatters, is given by the expression $Prob(\Delta s) \sim \exp(-\Delta s/\lambda)$. The probability of finding a particle in a pitch angle interval $d\mu$ where $\mu = \cos\theta$ is μ , and the time between collisions is $v|\mu|$ for particle velocity v and μ chosen randomly between -1 and $+1$. Since cross field diffusion is neglected, $\Delta x = \Delta s \cos\psi$. To take into account increased downstream scattering, we take $\lambda_{\circ,1} = 4\lambda_{\circ,2}$.

In the shock rest frame, the flow velocity (V_1, V_2) for upstream and downstream respectively, is parallel to the shock normal and the magnetic fields \mathbf{B}_1 and \mathbf{B}_2 are at an angle ψ_1 and ψ_2 to the shock normal respectively. We adopt a geometry with x in the flow direction, positive downstream, $\mathbf{B}_1, \mathbf{B}_2$ in the $x - y$ plane and directed in the negative x and y directions and only \mathbf{E}_z finite and in the positive z direction. A relativistic transformation is performed to the local fluid frame each time the particle scatters across the shock.

Now, for the transformations between the shock frame and the de Hoffmann-Teller frame, we need to boost by a V_{HT} speed along the shock frame where, V_{HT} is equal to $V_1 \tan\psi_1$. The transformation to the de Hoffmann-Teller frame though, is only possible if V_{HT} is less or equal to the speed of light. This means

that $\tan\psi_1 \leq 1$ (sub-luminal case). The particles ($\sim 10^5$) of a weight equal to 1.0, are injected far upstream at a constant energy of high gamma, which supposes that a pre-acceleration of the particles has already taken place, following for example the astrophysical scenario of Gallant and Achterberg (1999) and as discussed in more detail in Meli and Quenby (2002a). The particles are left to move towards the shock, along the way they collide with the scattering centers and consequently as they keep scattering between the upstream and downstream regions of the shock (its width is much smaller than the particle's gyroradius) they gain a considerable amount of energy (see figures of the next section). For the case of highly relativistic flows, the definition of particle pitch angle diffusion is that the scattering is limited within an upstream frame angle $\sim 0.1/\Gamma$ where, Γ is the upstream gamma, measured in the shock frame (Gallant and Achterberg, 1999) and investigated by Protheroe et al. (2002). This condition is also included in the current Monte Carlo for appropriate comparisons. The energy of the particle is kept constant at the scattering centers and only the direction of the velocity vector is randomized. We put forward a condition for large angle scattering to occur in Meli and Quenby (2002a), $r_{g,1} \leq \lambda_1/2\Gamma_1^2$ where the mean free path and gyroradius within the scatter centre, $r_{g,1}$, are measured in the upstream frame and will also consider this case as possible, but the reasoning, both for the sub-luminal and the super-luminal situations is modified. However, we note Achterberg et al. (2001) exclude large angle scatterings in an extensive investigation of a variety of models.

Provided the field directions encountered are reasonably isotropic in the shock frame, we are about to show $\tan\psi_1 = \Gamma_1^{-1}\tan\psi_s \sim \Gamma_1^{-1} \sim \psi_1$ where '1' and 's' refer to the upstream and shock frames. Now, $V_1 = c(1 - 0.5\Gamma_1^{-2})$ while, a particle at velocity c in the upstream frame starting along the shock normal, needs a deflection of Γ_1^{-1} radians to be reduced to V_1 resolved in the shock normal direction and hence, be overtaken by the shock. This angle is the limit of gyration allowed in the upstream field perpendicular to the shock normal before some large angle scatter must take place. If t_u is the time to the scatter and ω_\perp is the perpendicular gyrofrequency, the angular deflection limit is $\omega_\perp t_u = \Gamma_1^{-1}$ where, $\omega_\perp = u_\perp/r_{a,\perp,1}$ and $u_\perp = c\psi_1$. Then the allowed distance before large angle scatter is $\lambda_\parallel = ct_u \leq r_{a,\perp,1}$. This means the Larmor radius of the high field 'bullet' scatter centre is, $r_{g,1} \leq r_{a,\perp,1}/\Gamma_1^2$ using the previous condition, which requires field strength regimes as discussed in Meli and Quenby (2002a) for possible GRB situations.

Between the 'i th' and 'i+1 th' scattering, we check for a shock crossing up to down via ($c = 1$ units)

$$\Delta x_s^{i+1} = \Gamma_1(\Delta x_i^i + V_1|\frac{\Delta x_1^i \sec\psi_1}{v_1 \cos\theta_1}|) \quad (5)$$

$$\Delta t_s^{i+1} = \Gamma_1(|\frac{\Delta x_1^i \sec\psi_1}{v_1 \cos\theta_1}| + V_1\Delta x_1) \quad (6)$$

where ψ_1 is measured in the upstream frame. Defining \mathbf{B}_s and \mathbf{E}_s in the shock normal frame with compression ratio r , we arrive at upstream frame quantities; $B_{1,x} = B_{s,x}$, $B_{1,y} = \Gamma_1(B_{s,y} + V_1 E_{s,z})$, $E'_{1,z} = 0$ where $E_{s,z} = V_1 B_s \sin\psi_{1,s}$. Also $\tan\psi_1 = \Gamma_1^{-1} \tan\psi_s$. Note the high relative velocity of the frames in the x direction induces an electric field which via a back induction suppresses the y component of \mathbf{B} and swings the field lines towards the x axis in the plasma frame.

Physically, for the occurrence of a shock crossing the conservation of the adiabatic invariant in the de Hoffman-Teller frame is used. However, to get into this frame we need all components of momentum and so need to assign a particle phase angle ϕ at random. Then, in $m = 1$ units, the momentum components for particle mass γ are,

$$p_{1,x} = \gamma_1 v_1 \cos\theta_1 \cos\psi_1 - \gamma_1 v_1 \sin\theta_1 \cos\phi_1 \sin\psi_1 \quad (7)$$

$$p_{1,y} = \gamma_1 v_1 \cos\theta_1 \sin\psi_1 + \gamma_1 v_1 \sin\theta_1 \cos\phi_1 \cos\psi_1 \quad (8)$$

$$p_{1,z} = \gamma_1 v_1 \sin\theta_1 \sin\phi_1 \quad (9)$$

A two stage transform is the initiated, first to the shock frame,

$$\gamma_s = \Gamma_1(\gamma_1 + V_1 p_{x,1}) \quad (10)$$

$$p_{s,x} = \Gamma_1(p_{x,1} + V_1 \gamma_1) \quad (11)$$

$$p_{s,y} = p_{y,1} \quad (12)$$

$$p_{s,z} = p_{z,1} \quad (13)$$

A transformation is now made into the de Hoffmann-Teller frame with a boost along the negative y axis with $V_{HT} = V_1 \tan\psi_1$. Then in this new frame, the B components become $-B_{HT,x} = \Gamma_{HT}(-B_{s,x} - V_{HT} E_{s,z})$, $B_{HT,y} = B_{s,y}$ and hence $\tan\psi_{HT,1} = \Gamma_{HT,1} \tan\psi_1$. Here the field lines are swept towards the transformation velocity in the y direction under frame transform. Energy and the y component of momentum are then transformed into the de Hoffmann-Teller frames according to, $\gamma_{HT} = \Gamma(\gamma_s + V_{HT} p_{s,y})$ and $p_{HT,y} = \Gamma_{HT}(p_{s,y} + V_{HT} \gamma_s)$ allowing the particle pitch angle to be obtained from $\cos\theta_{HT} = \mathbf{p} \cdot \mathbf{B}/pB$. Then the particle that crosses the shock from upstream, is transmitted only if its pitch angle is less than the critical pitch angle:

$$\theta_c = \arcsin \sqrt{\frac{\mathbf{B}_{HT,1}}{\mathbf{B}_{HT,2}}} \quad (14)$$

From the conservation of the first adiabatic invariant we can find the new pitch angle in the downstream frame and similar transformations allow the

particle scattering to be followed in this frame.

2.2 Super-luminal case

For the super-luminal case a variation of the computational model is applied, compared to the one depicted above. For this investigation we employ once again a Monte Carlo scheme and consider the motion of a particle of momentum p in the magnetic field \mathbf{B} . As we have mentioned, in the super-luminal situation it is not possible to transform to a single frame where $\mathbf{E}=0$ (de Hoffmann-Teller frame). Hence, for our investigation the most convenient frames of reference to use are the fluid frames (where still the electric field is zero) and the shock frame which we will use only as a frame to check whether upstream or downstream conditions apply. We inject $\sim 8 \times 10^5$ particles in order to keep reasonable statistics throughout the simulations. We consider large angle scattering, which is calculated in the respective fluid rest frames, based on the possible situation previously discussed. Also Bednarz and Ostrowski (1996) find that only in the large angle scattering case does a power law develop and thus this is the most favourable case to further investigate. It will at least yield a limit to the acceleration a super-luminal shock may provide. Initially we inject the particles 100λ from the shock and we follow their guiding center in the upstream frame as in the sub-luminal case until after the appropriate transformation to the shock frame the particle reaches the shock at $x_{sh} = 0$. At this juncture, there is no easy approximation to determine the probability of shock crossing or reflection. We change the model to following a helical trajectory, in the fluid frames upstream ('1') or downstream ('2') respectively, where the velocity coordinates of the particle are calculated in a three dimensional space as follows:

$$v_{x_1} = v_1 \cos\theta_1 \cos\psi_1 - v_1 \sin\theta_1 \cos\phi_1 \sin\psi_1, \quad (15)$$

$$v_{y_1} = v_1 \cos\theta_1 \sin\psi_1 + v_1 \sin\theta_1 \cos\phi_1 \cos\psi_1 \quad (16)$$

and,

$$v_{z_1} = -v_1 \sin\theta_1 \sin\phi_1 \quad (17)$$

where θ_1 is the pitch angle and ψ_1 is the angle between the magnetic field and the shock normal.

We follow the trajectory in time, using $\phi_1 = \phi_o + \omega t$, where $\phi_1 \in (0, 2\pi)$ and t is the time from detecting shock presence at x_{sh}, y_{sh}, z_{sh} by using,

$$dx = x_{sh} + v_{x_1} \delta t \quad (18)$$

$$dy = y_{sh} + v_{y_1} \delta t \quad (19)$$

and,

$$dz = z_{sh} + v_{z_1} \delta t \quad (20)$$

assuming that $\delta t = r_g/Hc$, where r_g is the Larmor radius, $H \geq 100$. The particle's gyrofrequency ω is given by the relation:

$$\omega_1 = \frac{e|\mathbf{B}_1|}{\gamma_1} \quad (21)$$

\mathbf{B}_1 is the magnetic field, γ_1 is the particle's gamma and e is its charge in gaussian units. For a matter of convenience though, the last relation is transformed in units of c/sec . All the above relations apply to the downstream case by only changing respectively the signs from 1 to 2, and all the calculations are performed in the upstream or downstream frames. Because of the peculiar properties of the helix we need to establish where a particle -in the upstream frame- of a particular θ, ϕ first encounters the shock. To establish when this happens, we choose to go back a whole period,

$$T_1 = \frac{2\pi}{\omega_1} \quad (22)$$

by reversing signs of the helix velocity coordinates and keep checking throughout the simulation to see if the particle's trajectory encounters the shock again. The starting point for transforming to the downstream frame is the *furthest* upstream shock crossing. After making the suitable relativistic transformations to the downstream fluid frame by calculating the (x_2, y_2, z_2, t_2) and $(v_{x_2}, v_{y_2}, v_{z_2})$ coordinates, the momentum P_2 and the gamma γ_2 of the particle, we follow the trajectory of the particle for a whole downstream period,

$$T_2 = \frac{2\pi}{\omega_2} \quad (23)$$

checking to see whether the particle meets the shock again, by transforming to the shock frame. If the particle meets the shock then the suitable transformations to the upstream frame are made again and we follow the particle's trajectory as described above. If the particle never meets the shock, than its guiding center is followed, the same way as mentioned earlier for the upstream side after the injection and it is left to leave the system if it reaches a well defined E_{max} momentum boundary or, a spatial boundary of 100λ .

3 Results

In this section we present results of the simulations described above. We show similar figures regarding the acceleration time decrease, mean energy gain, spectral shapes and angular distributions for both sub- and super-luminal situations. First, the code runs have been tested in the non-relativistic and mild relativistic regime using $V_1 \sim 0.1c-0.6c$ and are found to be in accordance with non-relativistic theory and mild relativistic theoretical predictions (e.g. Kirk and Schneider, 1987a,b). In the highly relativistic regime for the sub-luminal case, the Lorentz factors of the flow used are equal to 10, 50, 200, 500 and 990. It is presumed that the injected particles are already relativistic with gammas just higher than the flow gammas. The compression ratio, r , has values of 3 and 4. The value of $r=3$ is expected to mimic the physical condition of an ultra relativistic gas. The value $r=4$ corresponds to the extreme hydrodynamic limit, where the magnetic field pressure is unimportant, but the shock speed in the upstream frame tends to c . However we will see from the figures that the value 3 or 4 does not alter the results (possibly due to the mildly-relativistic nature of the downstream plasma).

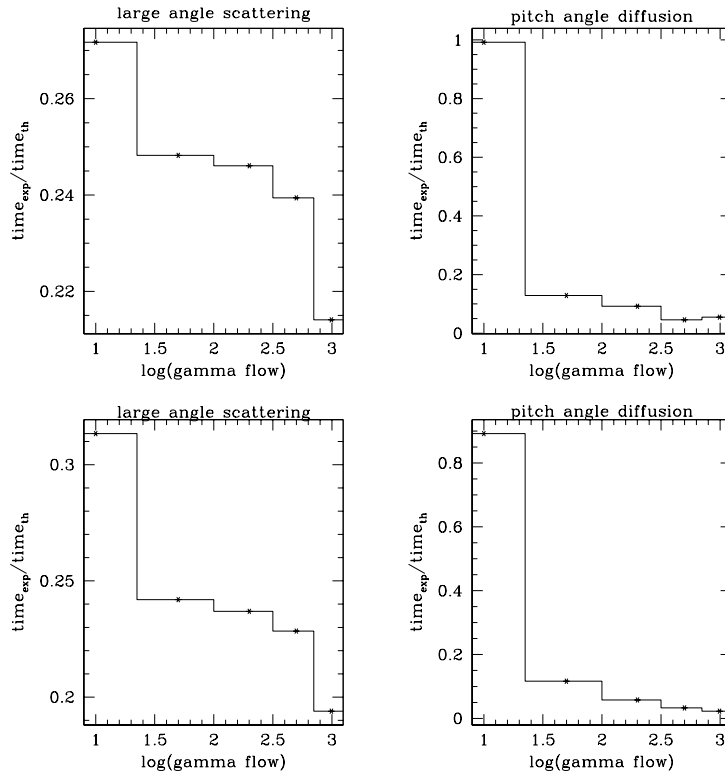


Fig. 1. The ratio of the computational time to the theoretical acceleration time constant versus the logarithm of the upstream gamma flow. Measurements are made at the de Hoffmann-Teller frame. The top plots show the acceleration time decrease in the case of the large angle scattering (left), pitch angle diffusion (right), for $\psi_1 = 15^\circ$, while the bottom ones are for $\psi_1 = 35^\circ$.

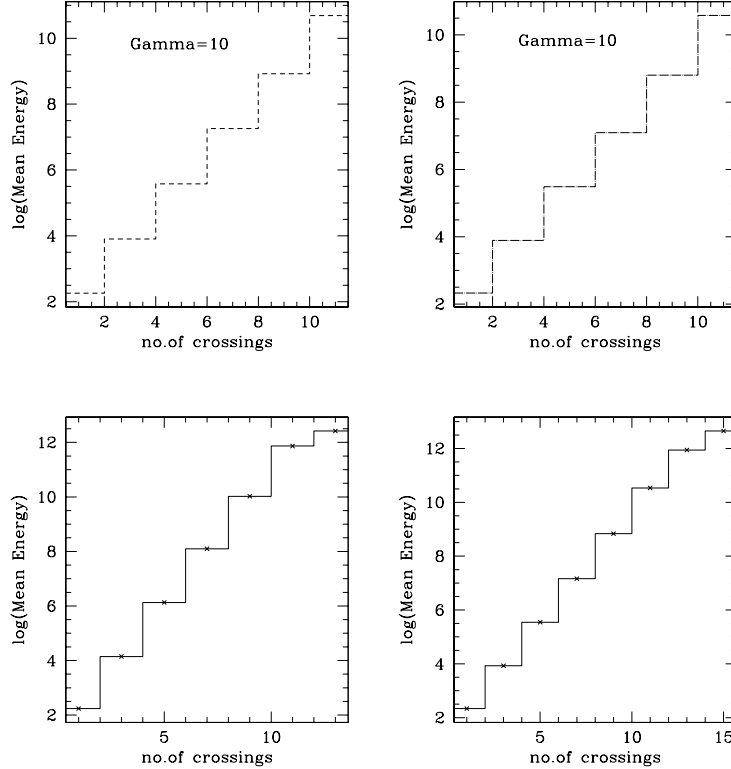


Fig. 2. The logarithm of the mean-energy gain of particles versus the number of shock crossings (1-3-5-7-9-11) for $\Gamma=10$ and $r=4$. Top plots: Large angle scattering, $\psi=15^\circ$ (left), $\psi=35^\circ$ (right). Bottom plots: Pitch angle diffusion, $\psi=15^\circ$ (left), $\psi=35^\circ$ (right). We observe the Γ^2 gain factor between the 1st and 3rd shock crossing (one cycle) and the efficient energy multiplication in subsequent crossings.

Two sub-luminal inclination cases are studied, equal to 15° and 35° . Particles are injected isotropically at 100λ upstream in the shock frame and when they reach the spatial boundary placed at $100\lambda_{\parallel}$ downstream they exit the simulation for the large angle case. We apply large angle and pitch angle scatters. For pitch angle scatter, the stability of the results against boundary position enabled a suitable downstream exit to be chosen (1000λ) where here, λ is the distance between scatterings. The mean free path (λ), is chosen to have the value of $\lambda \sim 20r_g$, close to the value that Quenby and Lieu (1989) used, based on a summary of interplanetary transport simulations referring to the only astrophysical plasma where we have any detailed knowledge of the magnetic field properties and performed by Moussas et al., 1992 (and references therein), but in most investigations it is only the ratio of up/down stream mean free paths and their ratio to the spatial boundary which matters. The momentum boundary is equal to $E_o 10^{14}$, where E_o is equal to the initial energy of the particle at the injection. For oblique sub-luminal shocks, we show in figure 1 the ratio of computational acceleration time to the analytic non-relativistic time constant, versus the logarithm of the upstream flow gammas used. The measurements are all made in the de Hoffmann-Teller frame as in

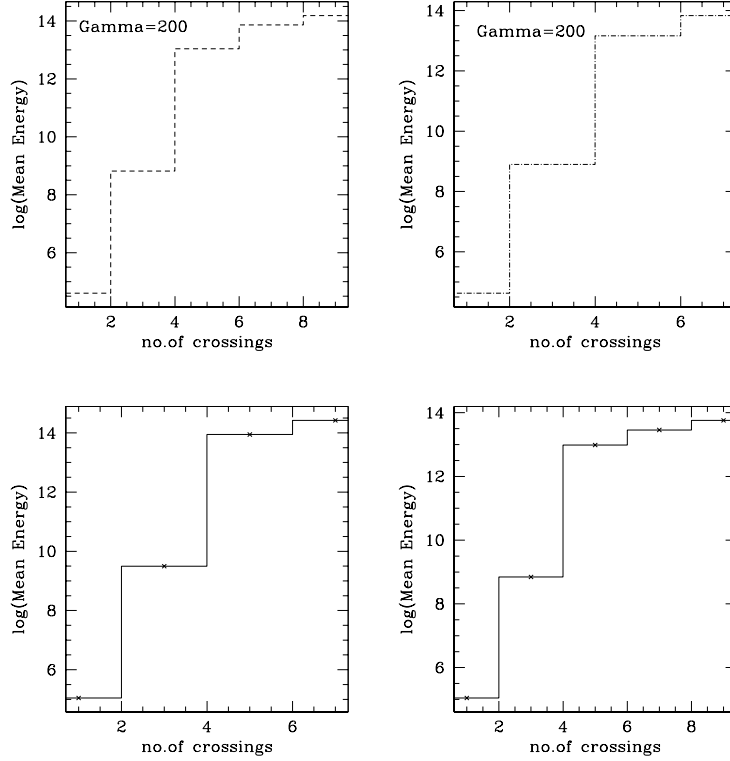


Fig. 3. The logarithm of the mean-energy gain of the particles versus the number of shock crossing (1-3-5-7) for $\Gamma=200$. Top plots: Large angle scattering, $\psi=15^\circ$, $r=4$ (left), $r=3$ (right). Bottom plots: Pitch angle diffusion, $\psi=35^\circ$, $r=4$ (left), $r=3$ (right). We observe the Γ^2 gain factor between the 1st and 3rd shock crossing and the efficient energy multiplication in subsequent crossings.

Lieu et al. (1994) where, it was found that this was a relevant frame to observe acceleration 'speed-up'. Then the non-relativistic acceleration time is,

$$\tau = \frac{3}{V_1 \cos \psi_1 - V_2 \cos \psi_2} \left(\frac{K_{n,1}}{V_1 \cos \psi_1} - \frac{K_{n,2}}{V_2 \cos \psi_2} \right) \quad (24)$$

When considering pitch or small angle scattering, the value of λ_{\parallel} employed is that for $\sim \pi/2$ scatter after random pitch change so that, $\lambda_{\parallel} = (\pi^2/4)(\lambda/\delta\theta^2)$ where λ is the distance between $\delta\theta$ collisions. We observe a significant acceleration time decrease of a factor $\sim 5-10$, which is comparable to that of the parallel shock 'speed up' found in Ellison et al. (1990) and Meli and Quenby (2002a). Basically, this 'speed up' effect observed is due to the Γ_1 energy increase each shock crossing, Γ_1^2 per cycle although it can be reduced by the very small pitch angles the particle may have in the small angle case as it crosses the shock upstream to downstream. In figures 2-4 the mean energy gain per crossing is presented for large angle scattering and pitch angle diffusion, with ψ_1 equal to 15° , 35° , $r=4$ and $r=3$ and $\Gamma = 10, 200$ and 990 . Particle energy is measured in γ units and so the plots are independent of mass and sign of

charge. The relative independence on r but the similarity in the trend from Γ^2 to Γ in energy dependence and finally 'saturation' found in the parallel case (Meli and Quenby, 2002a) are seen. The gain per crossing falls off noticeably faster as Γ_1 increases.

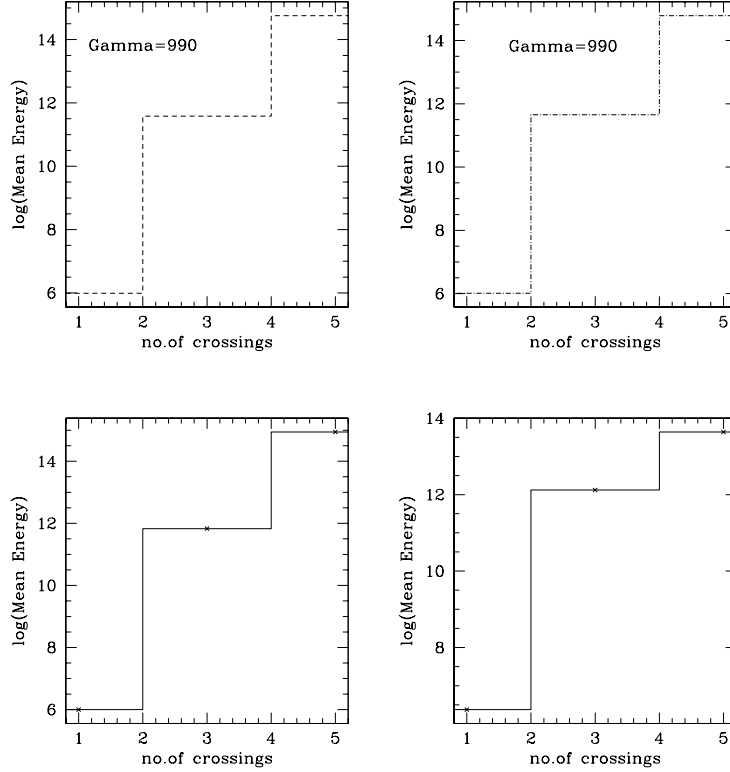


Fig. 4. The logarithm of the mean-energy gain of the particles versus the shock crossing (1-3-5) for $\Gamma=990$. Top plots: Large angle scattering, $\psi=15^\circ$ and $r=4$ (left), $r=3$ (right). Bottom plots: Pitch angle diffusion, $r=4$, $\psi=15^\circ$ (left), $\psi=35^\circ$ (right).

It must be emphasized that a full model would include loss processes which, would limit the maximum Γ obtainable. Note that proton energies $\sim 10^{20}$ eV can be reached in all models computed before the saturation sets in, provided faster loss mechanisms are not present. This is despite the relatively small amount of upstream deflection allowed before particles are swept downstream on all cycles except the first which, limits the first order 'Fermi' gain available (see Gallant and Achterberg, 1999, where the full Γ_1^2 factor requires isotropization in each frame). Rather different spectra shapes are seen in figures 5-8 for $\Gamma=10, 50, 500$ and 990 , depending on whether it is pitch angle or large angle scattering, at $\psi_1 = 15^\circ$ and $\psi_1 = 35^\circ$. The sensitivity to downstream boundary position has been checked up to a distance $r_b = 2 \cdot 10^5 \lambda$ where, λ is distance between small angle scattering for this model.

The plateau-like shapes are again prominent and more 'disrupted', compared to parallel shock cases found in the similar computations of Meli and Quenby (2002a), for large angle scatter. In the case of pitch angle diffusion the shapes

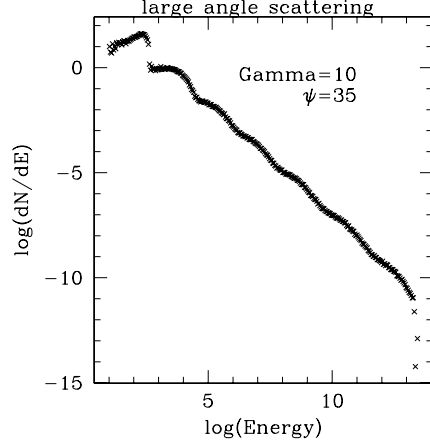


Fig. 5. Spectral shape for upstream gamma flow equal to 10, large angle scattering, $r=4$ and $\psi=35^\circ$. We observe the smoothness of the spectral shape compared to larger upstream gammas.

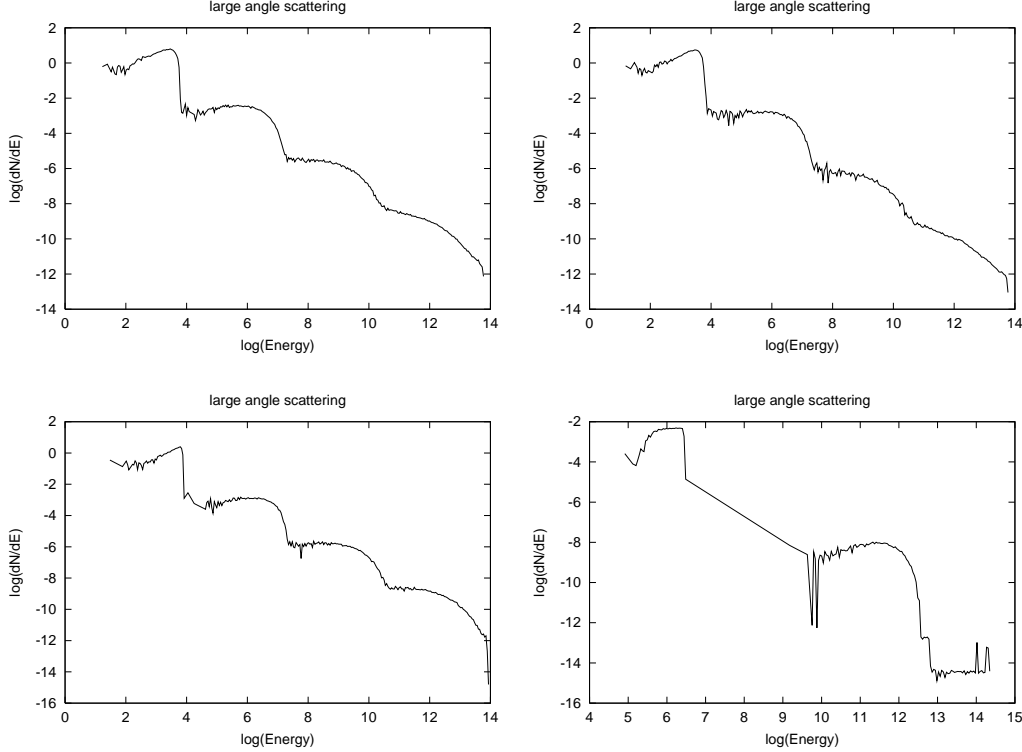


Fig. 6. Top plots: Spectral shapes for upstream gamma flow equal to 50 and large angle scattering. $\psi=15^\circ$, $r=4$ (left), $r=3$ (right). Bottom plots: Gamma=50 (left), 990 (right), $r=4$, $\psi=35^\circ$.

are much smoother, particularly at lower Γ_1 . The disrupted shapes are probably due to high anisotropy allowed in some situations. We qualitatively understand the spectral shapes in terms of each plateau exhibiting the acceleration gain in one shock cycle, down to up to down, with a Γ_1^2 factor boosting energy, followed by a high probability of loss downstream due to the beaming of

the particles away from the shock. Examples of the beaming are presented in figure 9 where, we see the angular distributions of the transmitted particles at the shock front in the de Hoffmann-Teller frame. We only show particles which have just crossed the shock, not the complete, time averaged, distribution function. The observed effect is due to the anisotropies in pitch angle space expected for highly relativistic flows, which are in accordance with lower Γ_1 results of Ellison et al., (1990) and Lieu et al., (1994).

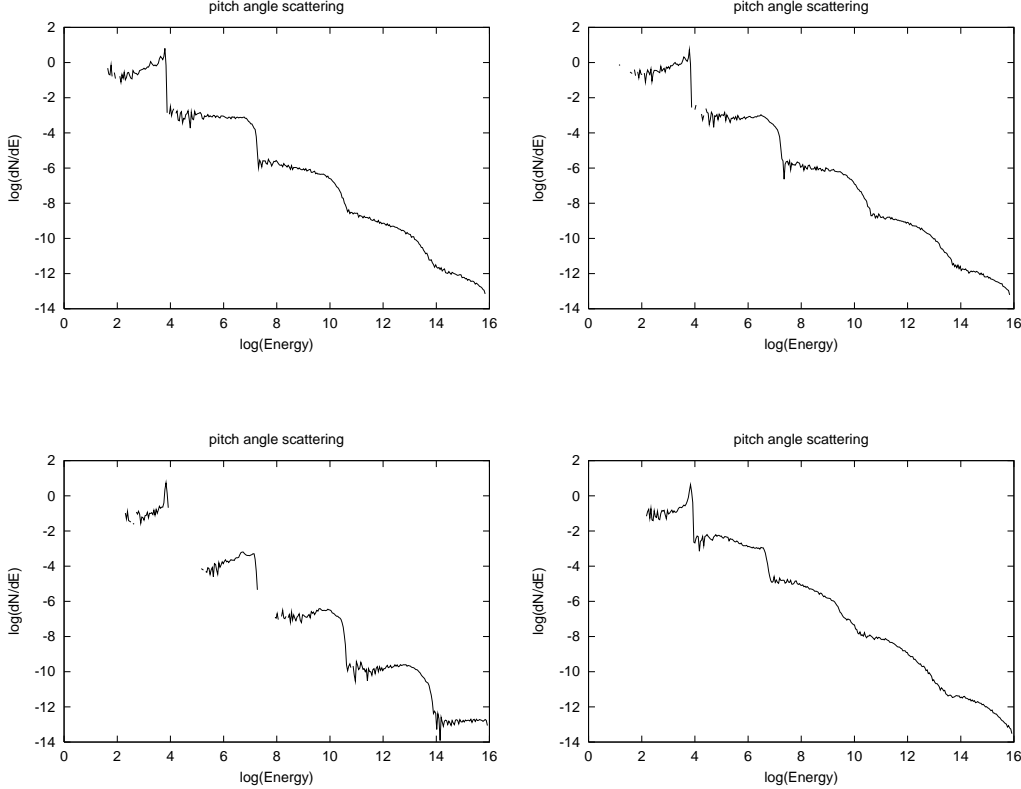


Fig. 7. Spectral shapes for pitch angle diffusion, for upstream $\Gamma=50$. Top plots: $\psi=15^\circ$, $r=4$ (left), $r=3$ (right). Bottom ones: $\psi=35^\circ$, $r=4$ (left), $r=3$ (right).

These results show that, due to very relativistic velocities the distribution functions are very anisotropic and so the spatial diffusion approximation cannot apply. In figures 10-11 we present results for the super-luminal case, where $\psi_1 = 48^\circ$ and 75° and Lorentz factors range from 10 to 40, expecting to apply in the relativistic flows of AGN environments. The compression ratio is equal to 4 and large angle scattering is used.

To obtain the spectral shapes for the accelerated particles as the trajectories are followed during the simulations, we add the momentum of each particle in the corresponding bin every time the particle crosses the shock as before to obtain the mean energy gain and distribution function. We observe that the spectral shape falls away from a power law and descends rapidly to an upper cut off which is expected, because the particles are swept away by the flow

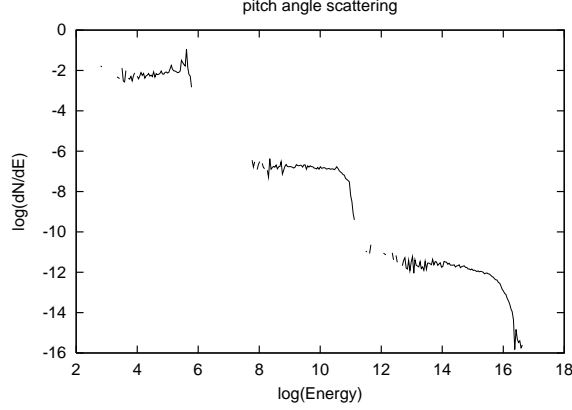


Fig. 8. Spectral shapes for $\Gamma = 500$, $\psi=15^\circ$, $r=4$ and pitch angle diffusion.

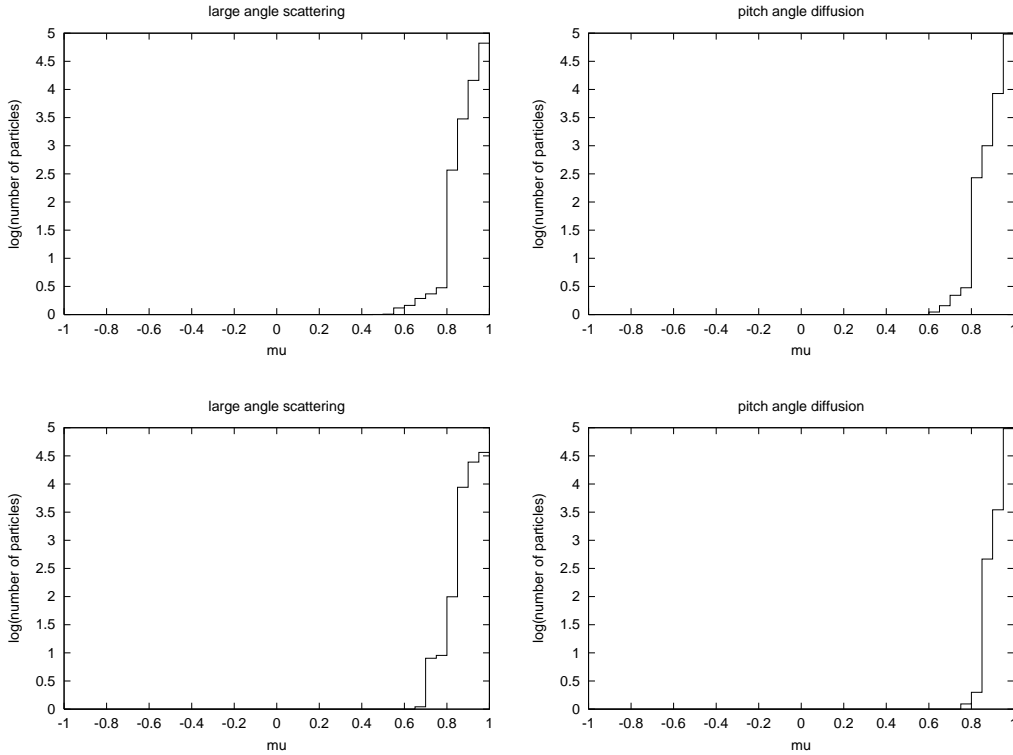


Fig. 9. The angular distribution of the logarithm of the number of transmitted (just crossed the shock) particles versus $\mu = \cos\theta$ at the de Hoffmann-Teller frame. Top plots: Upstream flow $\Gamma=200$ $\psi=15^\circ$ and $r=4$. Bottom plots: Upstream flow $\Gamma=990$, $\psi=35^\circ$ and $r=4$. In both cases we observe the strong 'beaming' of the particles' distribution.

after one cycle and have a very limited chance of return upstream, especially due to the high field inclination to the shock normal.

In the lower plots of figure 11, the energy gain of the particle is shown, versus the number of the helix-trajectory shock crossings for Lorentz factor 10 and $\psi_1 = 48^\circ, 75^\circ$ between the magnetic field and the shock normal. It is seen

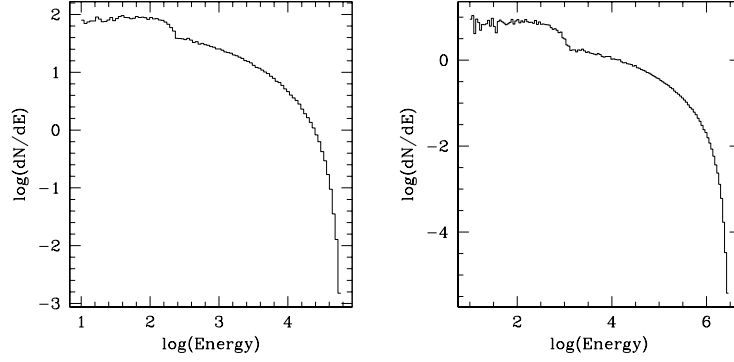


Fig. 10. Spectral shape for the super-luminal case, in the shock frame at the downstream side for $\Gamma=10$ and $\psi=48^\circ$ (left), $\Gamma=30$ and $\psi=75^\circ$ (right).

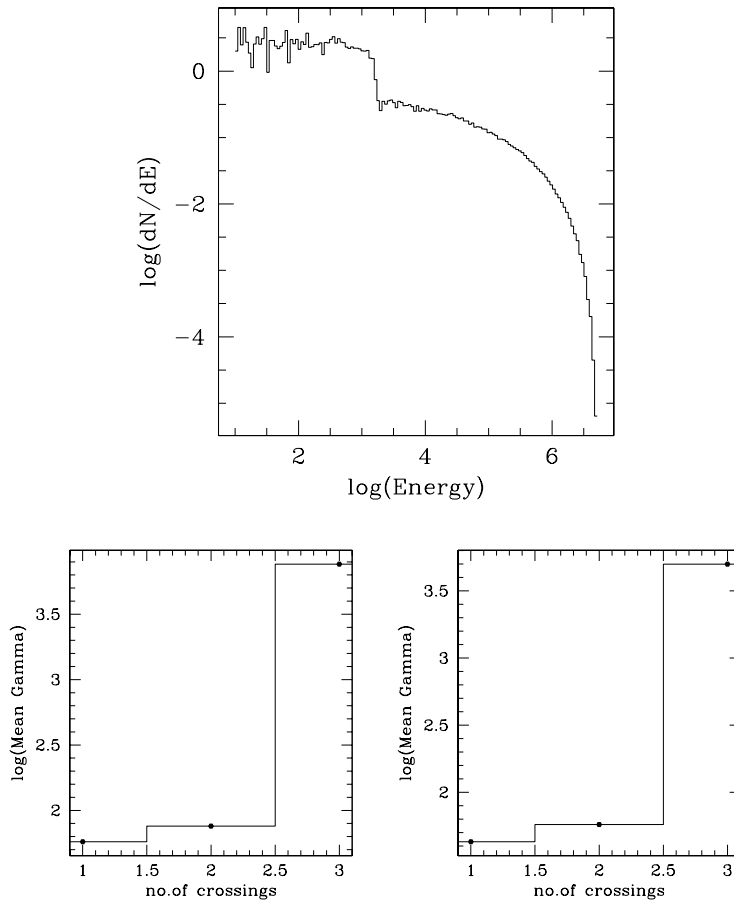


Fig. 11. Top plot: Spectral shape for the super-luminal case in the shock frame at the downstream side for $\Gamma=40$ and $\psi = 75^\circ$. We observe a structure at the beginning of the spectrum -near the injection point- and a cut off at high energies, compared to typical diffusive shock acceleration spectra. Bottom plots: Energy gain versus number of shock crossings (1-2-3) of the particle's helix trajectory for $\Gamma=10$, $\psi=48^\circ$ (left) and $\psi=75^\circ$ (right).

that after the 3rd crossing (after one cycle) the particle gains a considerable amount of energy ($\sim \Gamma^2$), but further gain is limited due to the fact that the particles are swept away by the flow very rapidly with no chance of 're-cycling' the shock again. Our calculations show that $\sim 60\%$ of the particles cross the shock three times (upstream \rightarrow downstream \rightarrow upstream \rightarrow downstream). It is possible to conclude that 'one-shot' drift acceleration has taken place, that is on one up to down crossing and there is energy increase as expected from drift in the shock frame electric field under the magnetic field gradient. Some particle return upstream has been possible under the action of large angle, downstream scattering. However this return flux is so limited that a power law spectrum cannot develop and a cutoff is soon reached. Computational time limitations have currently prevented an extension of the modeling to higher Γ flows and pitch angle scattering models for the super-luminal case.

4 Discussion and Conclusions

Oblique particle shock acceleration simulations for sub-luminal and super-luminal cases have been presented. High gamma upstream flows have been used ranging from $\Gamma=10$ up to $\sim 10^3$. The results found are important in answering questions concerning the efficiency and relativistic effects of first order Fermi acceleration. A major finding of both this work and the companion paper (Meli and Quenby, 2002a), is that in contrast to parallel shocks with small angle scattering, all other types of shocks and scattering models do not yield smooth, power law spectra at the shock in the $\Gamma \gg 1$ regime, even though subsequent smoothing during particle escape may arise. Reasons for this will be re-iterated later. However, sub-luminal, inclined relativistic shocks provide spectra more extended in energy and therefore more approximating to a power law distribution than super-luminal shocks, the latter exhibiting a pronounced high energy cutoff feature. The result that up to 3 crossings of the shock can often occur in the adopted large angle scattering model implies that the super-luminal case is not simply 'one-shot' shock drift. However the large gain crossing 2 \rightarrow 3 followed by loss to the system can well be described as the energy gain experienced on the last shock drift pass through the discontinuity standing out from the smaller, average diffusive gain.

Concerning the important 'speed up' effect in the sub-luminal case, this appears to be due to a combination of Γ^2 or Γ energy gain and the anisotropic angular distributions at the shock front (Ellison et al., 1990) which as we showed, is confined to a very small angle transmission cone. Thus, only a narrow range of pitch angle particles return to the shock and are 'counted' for the acceleration time calculation, as the ones with larger pitch angles are lost downstream. If the particle distribution is made isotropic each side of the shock before re-crossing, the energy gain per cycle is $\sim \Gamma_1^2$ Quenby and

Lieu (1989), but a distribution remaining anisotropic will experience less energy gain (Gallant and Achterberg, 1999). Hence some part of the 'speed up' compared with the non-relativistic situation is expected to be connected with the un-allowed for energy enhancement. The anisotropy is of course linked to the 'beaming effect' found also in mild relativistic cases, in accordance with Peacock (1981) and Kirk and Schneider (1988). Lieu and Quenby (1990) and Lieu et al. (1994) note that the distribution of the particle's pitch angle is peaked towards the direction of the relativistic transformation to the de Hoffmann-Teller frame. In other words this beaming which enhances the number of particles close to the field line, may provide an additional reason for the decrease in acceleration time as the flow becomes more relativistic for both large angle and pitch angle diffusion. This 'speed-up' resembles a trend found in the parallel shock particle acceleration case. Furthermore, the last arguments could explain the prominent spectral 'plateau' shapes found in many oblique, sub-luminal and parallel shock cases where each shock cycle crossing seems to stand out *separately*. Enhanced single cycle acceleration is followed by large flux loss downstream, preventing statistical smoothing into a single power law accelerated spectrum.

The 'speed up' effect -which has also been observed in the mildly relativistic regime Quenby and Lieu (1989) and Ellison et al. (1990), is important for a complete understanding of particle acceleration to the highest energies. An understanding of this crucial effect is necessary in any explanation for the maximum energy that particles (protons, electrons, iron nuclei) can achieve in GRB fireballs, AGN hotspots, and pulsar ultra relativistic polar winds. For example results found in the previous sections dealing with the sub-luminal case for $\Gamma \sim 10^3$, show only few crossings are needed for the particle to achieve energies up to $10^{19} - 10^{20}$ eV, although for $\Gamma \sim 10$ more than ten crossings may be needed to gain such high energies. It is the competition between loss time and energy gain time which determines the maximum energy in many situations. Generally speaking the percentage increase of the maximum energy would depend on many factors. One of those is the velocity of the upstream flow. Also the dimensions of the shock could play a vital role in order to define the escape losses in a specific shock acceleration site. In addition another factor in the physical conditions which could alter the cosmic ray spectrum and decrease the spectral index is due to different energy losses occurring in the regime; for example the presence of high or low energy photons (Greisen-Zatsepin-Kuz'min cutoff effect²) or $\gamma - \gamma$ flux interactions³ in GRB will decrease the maximum energy of the particles. In the context of AGN it is well known

² This is called also the microwave background effect, where the interaction between the cosmic rays and the microwave background results in a cutoff in the energy spectrum of cosmic rays (Greisen 1966; Zatsepin-Kuz'min 1966)

³ If GRB high energy photons come from electron acceleration in the $\Gamma \sim 10^3$ regime, we might expect some 'structure' in the spectrum at the higher energies on any scattering model.

from a number of interesting papers such as Protheroe and Kazanas (1983) and Chakrabarti and Moltoni (1993) that a shock in the central engine of the accreting flow ($\Gamma \simeq 5 - 10$) is likely to appear and particle acceleration can consequently take place. Also there is observational evidence that a common feature of many AGN is the formation of one or two jets where shock formations should appear in conjunction with $\Gamma \sim 5 - 10$ flows. Thus, the computed flattening of the spectra -they are all flatter than a -2 power law- as well as the acceleration 'speed up', should have important consequences when compared with predictions and observational data, regarding for example, the photons produced by emission from electrons which can be accelerated at the shocks or produced from accelerated protons. GRB seem to be another potential candidate for the acceleration of Ultra High Energy Cosmic Rays (UHECRs), but the issue is debated by many workers. As we have mentioned Vietri (1995) and Waxman (1995), who have exploited the 'gamma-squared' factor energy gain of the particle, were first to predict theoretically that indeed UHECRs can be produced in GRB where a pre-acceleration of the particles has been implied. Briefly, we note that observationally there is very strong evidence that pulsars (e.g. PSR 1913+16, PSR 2127+11C) are capable of injecting continuously relativistic particles into the surrounding medium over their lifetime. While this plasma will probably be predominantly in the form of e^+e^- pairs created in the pulsar magnetosphere, it has been argued that pulsar winds must also contain ions in order to account for the electrical current required in the Crab Nebula (Hoshino et al., 1992; Gallant and Arons, 1994). The termination shock as the $\Gamma \sim 10^5$ flow meets the nebula is likely to be quasi-perpendicular and hence the super-luminal situation applies for the additional e^+e^- acceleration. The enhanced production of neutrinos in astrophysical sites such as in AGN and GRB is another consequence of the simulation findings of the 'speed up' effect and 'gamma squared' factor. Mastichiadis and Kirk (1992), Protheroe and Szabo (1992) and Vietri (1998) showed that the neutrino flux depends on the maximum energy attained from the primary protons, thus a decrease of the acceleration time constant could produce higher maximum energy limits for the accelerated particles and consequently an increase in the cutoff energy of the neutrino flux will be noted.

Acknowledgements

We would like to express our thanks to Prof. Drury and the unknown referee for valuable comments and suggestions.

References

Achterberg, A. A., Gallant, Y. A., Kirk, J. G. and Guthmann, A. W., 2001,

- MNRAS, 328, 393.
- Armstrong, T. P., and Decker, R. B., 1979, 'Particle Acceleration Mechanisms in Astrophysics' AIP Proc. No 55, p. 101.
- Axford, W. I., Leer, E. and Skadron, G., 1978, 15th ICRC Plovdiv, Bulgaria, 11, 132.
- Axford, W. I. 1981, 17th ICRC, Paris, 12, 155.
- Baring, M. G., Ellison, D. C. and Jones, F. C., 1994, ApJS, 90, 547.
- Baring, M. G., Ellison, D. C. and Jones, F. C., 1995, Adv. Sp. Res., 15, No 8/9, 397, COSPAR.
- Bell, A. R., 1978a, MNRAS, 182, 147.
- Bell, A. R., 1978b, MNRAS, 182, 443.
- Bednarz, J. and Ostrowski, M., 1996, MNRAS, 283, 447.
- Bednarz, J. and Ostrowski, M., 1998, Ph. Rev. Lett., 80, 3911.
- Begelman, M. C and Kirk, J. G., 1990, ApJ., 353, 66.
- Blandford, R. D., and Ostriker, J. P., 1978, ApJ. Lett., 221, L29.
- Chakrabarti, S. K., Moltoni, D., 1993, ApJ., 417, 671.
- Drury, L. O'C, 1983, Rep. Prog. Phys., 1, 973.
- de Hoffmann, F., Teller, E., 1950, Phys. Rev., 80, 692.
- Ellison, D. C., Jones, F. C., Reynolds, S.P., 1990, ApJ., 360, 702.
- Gallant, Y. A. and Arons, J., 1994, ApJ., 435, 230.
- Gallant, Y. A. and Achterberg, A., 1999, MNRAS, 305, 6.
- Greisen, K., 1966, Ph. Rev. Lett., 16, 748.
- Hoshino, M., Arons, J., Gallant, Y. A., Langdon, A. B., 1992, ApJ., 390, 454.
- Hudson, P. D., 1965, MNRAS, 131, 23.
- Jokipii, J. R., 1966, ApJ., 146, 480.
- Jokipii, J. R., 1982, ApJ., 255, 716.
- Jokipii, J. R. and Parker, E. N., 1969, ApJ., 155, 177.
- Kirk, J. G. and Schneider, P., 1987a, ApJ., 315, 425.
- Kirk, J. G. and Schneider, P., 1987b, ApJ., 322, 256.
- Kirk, J. G. and Schneider, P., 1988, A&A, 201, 177.
- Kirk, J. G. and Heavens, A. F., 1989, MNRAS, 239, 995.
- Krymsky, G. F., 1977, Dokl. Acad. Nauk., SSSR, 234, 1306.
- Lieu, R. and Quenby, J. J., 1990, ApJ., 350, 692.
- Lieu, R., Quenby, J. J., Drolas, B. and Naidu, K., 1994, ApJ., 421, 211.
- Lucek, S. G. and Bell, A. R., 1994, MNRAS, 268, 581.
- Mastichiadis, A., Kirk, J. G., 1992, High Energy Neutrino Astrophysics, p.63, World Scientific.
- Meli, A. and Quenby, J. J., 2002a, Ast.Part. Phys. (accepted).
- Moussas, X., Quenby, J. J., Theodossiou-Ekaterinidi, Z., Valdes-Galicia, J. F., Drillia, A. G., Roulias, D., Smith, E. J., 1992, Sol. Phys., 140, 161.
- Ostrowski, M., 1991, MNRAS, 249, 551-559.
- Peacock, J. A., 1981, MNRAS, 196, 135.
- Protheroe, R. J., Kazanas, D., 1983, ApJ., 265, 620.
- Protheroe, R. J., Szabo, A. P., 1992, Phys. Rev. Lett., 69, 2885.
- Protheroe, R. J., Meli, A., and A.-C. Donea, 2002, WISER 2002, Adelaide,

- Sp. Sc. Rev. (accepted).
- Quenby, J. J. and Lieu, R., 1989, *Nature*, 342, 654.
- Quenby, J. J. and Drolias, B., 1995, 24th ICRC Rome, 3, 261.
- Vietri, M., 1995, *ApJ.*, 453, 883.
- Vietri, M., 1998, *ApJ. Lett.*, 448, L105.
- Waxman, E., 1995, *Phys. Rev. Let.*, 75, 386.
- Zatsepin, G. T., Kuz'min, V. A., 1966, *JETP Let.*, 4, 78.